

# Characterization of a dielectric phantom for high-field magnetic resonance imaging applications

Qi Duan,<sup>a)</sup> Jeff H. Duyn, Natalia Gudino, Jacco A. de Zwart, and Peter van Gelderen  
*Advanced MRI Section, Laboratory of Functional and Molecular Imaging, National Institute of Neurological Disorders and Stroke, National Institutes of Health, Bethesda, Maryland 20892*

Daniel K. Sodickson and Ryan Brown  
*The Bernard and Irene Schwartz Center for Biomedical Imaging, Department of Radiology, New York University School of Medicine, New York, New York 10016*

(Received 10 April 2014; revised 28 July 2014; accepted for publication 27 August 2014; published 24 September 2014)

**Purpose:** In this work, a generic recipe for an inexpensive and nontoxic phantom was developed within a range of biologically relevant dielectric properties from 150 MHz to 4.5 GHz.

**Methods:** The recipe includes deionized water as the solvent, NaCl to primarily control conductivity, sucrose to primarily control permittivity, agar-agar to gel the solution and reduce heat diffusivity, and benzoic acid to preserve the gel. Two hundred and seventeen samples were prepared to cover the feasible range of NaCl and sucrose concentrations. Their dielectric properties were measured using a commercial dielectric probe and were fitted to a 3D polynomial to generate a recipe describing the properties as a function of NaCl concentration, sucrose concentration, and frequency.

**Results:** Results indicated that the intuitive linear and independent relationships between NaCl and conductivity and between sucrose and permittivity are not valid. A generic polynomial recipe was developed to characterize the complex relationship between the solutes and the resulting dielectric values and has been made publicly available as a web application. In representative mixtures developed to mimic brain and muscle tissue, less than 2% difference was observed between the predicted and measured conductivity and permittivity values.

**Conclusions:** It is expected that the recipe will be useful for generating dielectric phantoms for general magnetic resonance imaging (MRI) coil development at high magnetic field strength, including coil safety evaluation as well as pulse sequence evaluation (including  $B_1^+$  mapping,  $B_1^+$  shimming, and selective excitation pulse design), and other non-MRI applications which require biologically equivalent dielectric properties. © 2014 American Association of Physicists in Medicine. [<http://dx.doi.org/10.1118/1.4895823>]

Key words: high-field MRI, wavelength effects

## 1. INTRODUCTION

At high magnetic field strength (3 T or higher) and correspondingly high Larmor frequency for  $^1\text{H}$  magnetic resonance imaging (MRI), the wavelength in typical tissues can be shorter than the human body. As a result, both the radio frequency (RF) transmit field (the  $B_1^+$  field) and the electrical field (the  $E$  field) become increasingly dependent on the dielectric properties of the object. For proper RF coil design and safety evaluation, the object, therefore, has to be taken into account. It is likewise desirable to characterize pulse sequences (such as  $B_1^+$  mapping and tailoring techniques<sup>1</sup>) in a phantom with biologically equivalent tissue properties. Additionally, both the spatial distribution and intensity of the heating pattern associated with RF deposition are related to the dielectric properties of the heated object. As a result, dielectric phantoms have been utilized to assess RF coil safety by, for example, measuring local heating during RF application using MRI thermometry.<sup>2-4</sup> Similarly, a biologically equivalent phantom is an essential fixture for coil array bench development (i.e., tuning, matching, and decoupling) and can also be of value for non-MRI RF

applications, such as safety tests for wireless devices, e.g., cellular phones.

To begin, we review the desired characteristics of the dielectric phantom. The phantom must be MRI-visible to allow imaging experiments. Typically this criterion implies a water-based phantom with reasonable  $T_1$  relaxation and  $T_2$  decay times. The conductivity ( $\sigma$ ) and (relative) permittivity ( $\epsilon_r$ ) must be matched to desired values at a particular Larmor frequency. Biologically relevant conductivity ranges from  $\sim 0.1$  S/m for adipose tissue and bone to 2–6 S/m for cerebrospinal fluid (in the frequency range 150 MHz–4.5 GHz).<sup>5,6</sup> Common salt (NaCl) can be added to deionized water to raise its conductivity, while its relative permittivity can be reduced from the nominal value of  $\sim 80$  by adding materials with low dielectric constant, such as acrylic rods,<sup>1</sup> polyvinyl chloride,<sup>7</sup> polyethylene powder,<sup>8-11</sup> polyoxyethylene sorbitan monolaurate,<sup>12,13</sup> oil,<sup>14,15</sup> or sugar.<sup>16-18</sup> Due to their high heat diffusivity, traditional liquid-based phantoms are not suitable for RF coil safety evaluations. In this context, gel-based phantoms are favorable because heat diffusivity can be reduced to the order of a centimeter during a typical safety evaluation where the RF irradiation period is typically on the order of

hundreds of seconds. In addition, water-soluble ingredients are preferred to generate homogeneous solutions that do not require complex mixing procedures or toxic additives. Finally, the cost of the phantom is a rarely discussed but important consideration. A low cost recipe is desirable, particularly for large volume body-sized phantoms.

Here, we characterize and evaluate a sucrose–NaCl-based gel phantom material (alternatively called “dielectric simulator” in Refs. 12 and 13) which satisfies all of the above requirements to prepare phantoms with dielectric properties that mimic tissue. To date, despite the fact that dielectric properties for tissues at various frequencies are publicly available (e.g., <http://transition.fcc.gov/oet/rfsafety/dielectric.html>), the recipes in the literature are primarily limited to a handful tissue types, i.e., fixed conductivity–permittivity combinations. A recipe that covers all possible sucrose and NaCl concentrations and can match a wide range of desired dielectric properties is not available in public domain. The main goal of this work was to characterize the dielectric properties resulting from a range of sucrose–NaCl samples and subsequently generate a parametric recipe for phantom preparation that will be made available in public domain. Although the main focus was MRI applications, where the operating frequency is generally at or below 500 MHz, a wide frequency range (150 MHz–4.5 GHz) was explored such that the parametric recipe was valid for high frequency applications, such as dosimetry of cellular phones, medical applications of electromagnetic fields, and body centric wireless area network applications.

## 2. METHODS

### 2.A. Basic ingredients and general protocol

The five ingredients are described below. All ingredients are chosen for their low cost, water solubility, nontoxicity, and general availability, and are reported as a percentage, in terms of mass per unit water volume.

- Solvent: Deionized water.
- Ingredient to primarily control conductivity: American Chemical Society (ACS) grade NaCl [Sigma sodium chloride (ReagentPlus™ ≥99.5%) S9625-500G (Sigma-Aldrich, St. Louis, MO) was used initially and later replaced by sodium chloride, Crystal, Baker Analyzed ACS

Reagent, J.T. Baker® 3624-01 (MG Scientific, Pleasant Prairie, WI)].

- Ingredient to primarily control permittivity: Sucrose in the form of table sugar (Premium Pure Cane Granulated, Domino Foods, Inc., Brooklyn, NY).
- Preservative: Benzoic acid. Benzoic acid is a common preservative used in the food industry and naturally exists in some plant and animal species, such as cranberry. Benzoic acid A68-30 (Thermo Fisher Scientific, Inc., Waltham, MA) was used with a fixed concentration (0.1%).
- Gelling agent: Agar (Fluka Agar-Agar for Microbiology 05039-50G, Sigma-Aldrich, St. Louis, MO) with a fixed concentration (1.5%).

The general protocol to prepare the phantom samples is described below.

1. Measure all ingredients (water, NaCl, sucrose, benzoic acid, and agar).
2. Mix the ingredients in a container.
3. Evenly heat and stir the mixture until the solutes have dissolved completely and a uniform solution is observed, and a temperature of at least 60 °C is reached. (Care should be taken to minimize evaporative losses.)
4. Pour the mixture in a slow and controlled manner into the phantom container, such that air bubbles within the mixture are minimized.
5. Allow the phantom to naturally cool to room temperature.

### 2.B. Concentration matrix and recipe fitting

To investigate the effect of NaCl and sucrose on dielectric properties, one hundred and seventeen 250-ml phantom samples were prepared using the protocol above with the following range of ingredients: NaCl ranged from 0.90% to 3.61% at intervals of 0.23% and sucrose ranged from 15.6% to 189.4% at intervals of 21.7%. This collection of samples formed a 9 × 13 concentration matrix [as shown in Fig. 1(a)] which was designed to cover a reasonable range of biological dielectric properties.

A second set of samples was prepared over coarser intervals of NaCl and sucrose concentrations to explore the dielectric limits of the recipe, that is, the point at which the water is saturated with either ingredient. For this purpose, a set of one hundred 250-ml samples was prepared to cover a 10 × 10 matrix where NaCl ranged from 0% to 35.7% at intervals of



FIG. 1. (a) 9 × 13 phantom sample matrix, (b) experiment setup for dielectric property measurement.

3.97% and sucrose ranged from 0% to 207% at intervals of 23%. The dielectric properties of each sample were measured using an invasive probe from 150 MHz to 4.5 GHz in 5 MHz steps at approximately 21.8 °C [slim form model; Agilent 85070E dielectric probe with Agilent E5071C network analyzer, see Fig. 1(b)].

To generate a recipe for target dielectric properties at a given frequency, measurements of all 217 samples were fitted to a 3D polynomial using customized MATLAB software (version R2013b, with supporting parallel computing toolbox; Mathworks, Natick, MA), where the dimensions represent NaCl and sucrose concentrations and frequency. Polynomial fitting was chosen for several reasons: robustness to measurement noise, the feasibility to incorporate supplemental data points, and a parameterized output recipe that is convenient to distribute.

## 2.C. Recipe validation

To evaluate the validity and accuracy of the parametric recipe, phantoms were prepared with dielectric properties approximating average muscle tissue at 300 MHz (for proton MRI at 7 T) (phantom A,  $\sigma = 0.79$  S/m,  $\epsilon_r = 59$ ) and average brain tissue at 500 MHz (for proton MRI at 11.7 T) (phantom B,  $\sigma = 0.63$  S/m,  $\epsilon_r = 48$ ).<sup>5</sup> The dielectric properties of these two phantoms were measured and compared with the target values. To estimate the repeatability of the protocol, four separate samples were prepared with the same solvent concentrations (118% sucrose and 1.43% NaCl), whose dielectric properties were measured six times in total (three measurements on the first sample and one on each of the remaining three samples). The confidence intervals were estimated from the standard deviations of these measurements, which capture errors in the entire procedure, e.g., fitting inaccuracies, ingredient volume measurement errors, and errors associated with the dielectric probe measurements. Properties of the first 117 samples were remeasured after eight months to test stability. During this period, the samples were sealed in plastic containers and stored at room temperature. Finally, 99 samples were measured at 25.8 °C to attain a sense of the relationship between temperature and dielectric properties.

The range of dielectric properties allowed by the proposed set of ingredients is inherently limited primarily by sucrose solubility for low permittivity samples, NaCl solubility for high conductivity samples, and nominal water conductivity for low conductivity samples (particularly at high frequency). Correspondingly, we sought to explore the frequency range over which the developed recipe is able to replicate the target dielectric properties of various tissues. Target properties were calculated from 150 MHz to 4.5 GHz with a 5 MHz step size using the following web application: <http://niremf.ifac.cnr.it/tissprop/htmlclie/htmlclie.htm>. These dielectric values were compared to those achievable with the proposed recipe; the values were considered to be adequately matched if the discrepancy was less than 10%.

## 2.D. Relaxation time measurement

To investigate the compatibility of the gel mixture with MR imaging,  $T_1$  and  $T_2^*$  values were measured in nine phantoms on

a 7 T system (MAGNETOM, Siemens Healthcare). The nine phantoms consisted of a  $3 \times 3$  subset of the phantoms with the minimum, median, and maximum sucrose and NaCl concentration values from the original  $9 \times 13$  matrix.  $T_1$  was mapped using spin echo images with an inversion preparation and the following parameters:  $TE = 20$  ms,  $TR = 10\,000$  ms, and  $TI = 23, 50, 100, 200, 400, 600, 800, 1000,$  and  $9500$  ms. Signal intensities were fit to the function  $S(TI) = |S_0[1 - 2\alpha \exp(-TI/T_1) + \exp(-TR/T_1)]|$  using an unconstrained nonlinear optimization search algorithm in MATLAB, where  $S_0$  is the equilibrium magnetization and  $\alpha$  is the inversion efficiency.  $T_2^*$  was mapped by fitting the signal intensities from a series of gradient echo images to a monoexponential decay model  $S(TE) = A + S_0 \exp(-TE/T_2^*)$ , where  $A$  is the signal offset,  $TE = 2.28$ – $19.08$  ms with 3.36 ms steps.

## 3. RESULTS

The dielectric property measurements at 500 MHz are shown in Fig. 2, with each grid point representing a pair of sucrose and NaCl concentration values. Strong nonlinearity between solvent concentration and dielectric values can be observed, especially for the conductivity values ( $x$ -axis) due in part to the high sucrose-to-NaCl concentration ratio. Additionally, interdependence between solvent concentration and dielectric values was observed: NaCl concentration was proportional to conductivity and inversely proportional to permittivity, and sucrose concentration was inversely proportional to both conductivity and permittivity.

The following 3D polynomial orders were found to capture the data dynamics while reducing sensitivity to measurement noise: 7th order on sucrose concentration, 5th order on NaCl concentration, and 7th order on frequency. In addition, to avoid a result that was numerically dominated by one particular input variable while disregarding the others, all inputs (sucrose concentration, NaCl concentration, and frequency) were normalized to approximately unity before polynomial fitting was performed. The polynomial function shows good agreement

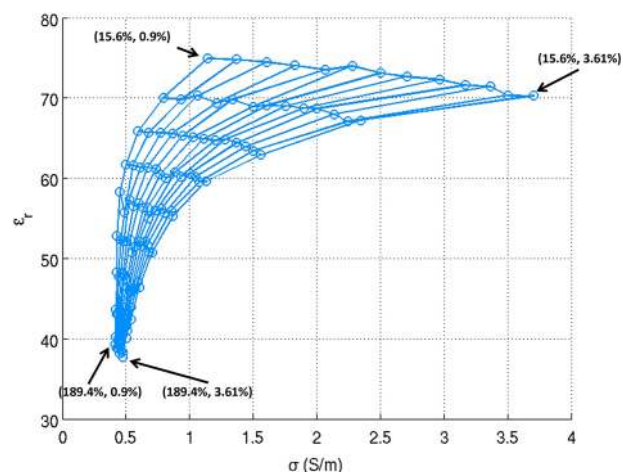


Fig. 2. Relative permittivity versus conductivity for the first 117 samples (in the  $9 \times 13$  matrix) prepared with linearly spaced solvent concentrations at 500 MHz. The concentrations for the corner points are given in the format of (sucrose concentration, NaCl concentration).



with the measured data (demonstrated in Fig. 3 at 500 MHz). This function is reimplemented in GNU Octave (<http://www.gnu.org/software/octave/>) and is available as a web application at our laboratory's public website (<http://www.amri.ninds.nih.gov/phantomrecipe.html>). For the purpose of brevity, the polynomial coefficients are omitted from the paper and are instead listed on the website, along with a MATLAB code example using the coefficients.

The ingredients for a phantom that simulates muscle tissue at 7 T (300 MHz) ( $\sigma = 0.79$  S/m,  $\epsilon_r = 59$ ) and average brain tissue at 11.7 T (500 MHz) ( $\sigma = 0.63$  S/m,  $\epsilon_r = 48$ ) are given in Table I. Note that the recipe predicts the total gel mixture volume, which is highly dependent on sucrose concentration and density.<sup>19</sup>

The dielectric properties were well matched to the targeted values with root-mean-squared errors less than 1.3% over the entire frequency range (150 MHz–4.5 GHz), with validation results at target frequencies shown in Table II. The differences between the measured and predicted values are less than twice the standard deviations of the repeated measurements (1.72% for relative permittivity and 1.68% for conductivity), which suggest that errors in the model prediction are comparable to those associated with phantom preparation and probe measurement. The samples demonstrated adequate stability over time; the root-mean-squared differences of measurements conducted eight months apart were 3.5% for permittivity and 2.2% for conductivity over the entire frequency range.

Note that while the ingredients were specified for muscle and brain tissue at 300 and 500 MHz, agreement between the measured and predicted values was maintained between 150 MHz and 4.5 GHz. While this provides evidence that the parametric recipe captures the behavior of the gel mixtures over a wide frequency range, the dielectric properties of a given gel mixture may change with frequency in a different manner than a given biological tissue. Therefore, it may be necessary to prepare a unique gel mixture to represent a given tissue at a given frequency.

The  $T_1$  and  $T_2^*$  values showed a strong inverse dependence on sucrose concentration and were largely independent of NaCl concentration. The  $T_1$  and  $T_2^*$  values are reported as mean  $\pm$  standard deviation across samples with three different NaCl

TABLE I. Recipes for tissue-mimicking phantoms used in the paper (normalized to 1000 ml water)

Ingredients	7 T muscle phantom (Phantom A)	11.7 T brain phantom (Phantom B)
Water (ml)	1000	1000
NaCl (g)	37.1	34.8
Sucrose (g)	964.3	1346.0
Agar (g)	15	15
Benzoic acid (g)	1	1
Total volume (ml)	1601.2	1842.3

concentrations (0.9%, 2.3%, and 3.6%). The  $T_1$  values were  $1785 \pm 37$ ,  $526 \pm 12$ , and  $386 \pm 3$  ms and the  $T_2^*$  values were  $47.1 \pm 1.4$ ,  $13.7 \pm 1.6$ , and  $6.1 \pm 0.2$  ms for samples with 15.6%, 102.4%, and 189% sucrose, respectively. Note that the  $T_1$  and  $T_2^*$  values were not intended to match those of a particular tissue. Nevertheless, they were measured to assure that the samples had appropriate relaxation characteristics for a wide range of MR experiments when using typical imaging parameters.

Figure 4 illustrates the shift in dielectric properties at 500 MHz corresponding to a 4 °C temperature change. The value shifted between 0.0024% and 6.92% for conductivity and between 0.16% and 5.6% for permittivity.

The dielectric property boundaries achievable, ranging from pure deionized water at one extreme to the maximum feasible concentration of either NaCl or sucrose at the other extreme, are plotted in Fig. 5 for a range of popular operating frequencies for high-field MRI (300 and 500 MHz) and cellular communication (1.9 and 2.4 GHz). The minimal conductivity is limited by that of distilled water, which increases substantially with frequency. For this reason, along with sucrose solubility limits, low conductivity tissues such as adipose cannot be mimicked with the developed recipe. Intermediate conductivity tissues can be achieved up to a cutoff frequency (e.g.,  $\sim 1.4$  GHz for muscle and gray matter), and high conductivity tissues such as cerebrospinal fluid can be achieved for the entire frequency range explored here. The frequency upper limits for various tissues are listed at <http://www.amri.ninds.nih.gov/phantomrecipe.html>. Finally, it is difficult to simultaneously

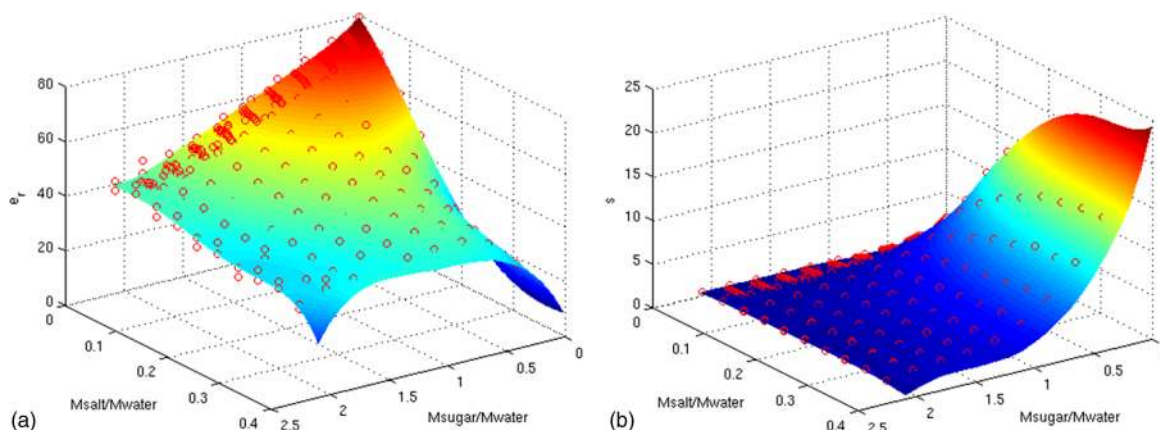


FIG. 3. The fitted results (surface) are well matched to the measured input data (circles) for (a) relative permittivity and (b) conductivity at 500 MHz using all the measurements.

TABLE II. Validation results for 300 MHz (7 T) muscle phantom A and 500 MHz (11.7 T) brain phantom B.

	Frequency	Measurement		Model prediction		Relative error (%)	
		$\sigma$ (S/m)	$\epsilon_r$	$\sigma$ (S/m)	$\epsilon_r$	$\sigma$	$\epsilon_r$
Phantom A	300 MHz	0.79	59.3	0.79	59.0	0.00	-0.51
Phantom B	500 MHz	0.64	47.8	0.63	48.4	-1.56	1.26

achieve high conductivity and low permittivity due to the effects of sucrose on conductivity, though this combination of properties is rarely encountered in human tissue.

#### 4. DISCUSSION

In this study, the relationship between dielectric properties and the NaCl and sucrose concentrations was studied at various frequencies by direct measurement in phantoms representing a range of biologically relevant properties. A complex relationship between the solute concentrations and the resulting dielectric properties was observed, thereby preventing accurate dielectric property prediction derived under the assumption of simple linear relationships between NaCl concentration and conductivity and between sucrose concentration and permittivity. This behavior was captured by the generic recipe, which was generated via 3D polynomial fitting of the measurement data. The resulting parametric recipe was made publicly available via a web application, which is expected to guide the preparation of dielectric phantoms.

It is worth noting that the nonlinear connection between sucrose and conductivity was of a much higher order than that was previously described in nonsoluble plastic powder-based phantoms,<sup>7,20,21</sup> which were primarily due to fractional concentration. This suggests that sucrose molecules affect ion transport or effective ion concentration in a superlinear manner. Such phenomenon has been previously reported by the

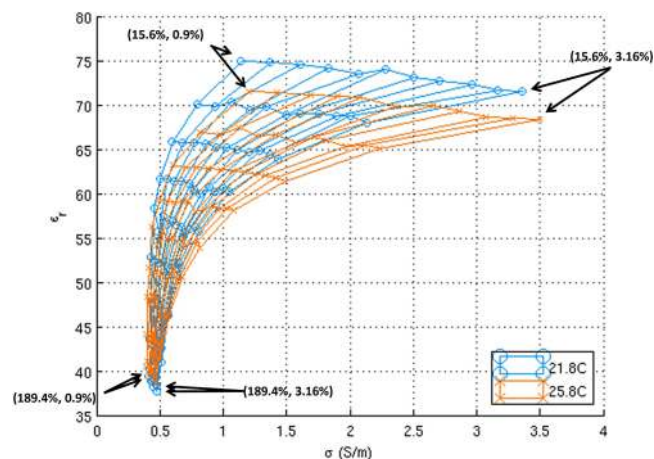


FIG. 4. Dielectric properties of 99 samples measured at 21.8°C (mesh with circles) and 25.8°C (mesh with crosses) at 500 MHz. The concentrations for the corner points are given in the format of (sucrose concentration, NaCl concentration).

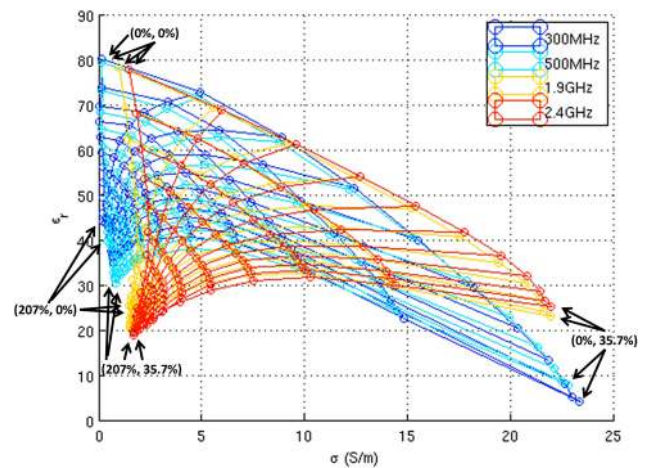


FIG. 5. Plot illustrating the boundaries of the recipe, which range from pure deionized water to the maximal NaCl and/or sucrose solutes for a range of high-field MRI (300 and 500 MHz) and cellular communication (1.9 and 2.4 GHz) frequencies. The concentrations for the corner points are given in the format of (sucrose concentration, NaCl concentration).

physical chemistry society<sup>22</sup> but has not been emphasized in the dielectric phantom literature.

While the goal of this study was to develop phantoms with specific dielectric properties rather than  $T_1$  and  $T_2$  values, relaxation properties are also key characteristics for MR compatibility. The relaxation times for the phantoms developed here were reasonable for most MRI applications, including  $B_1^+$  mapping and MRI thermometry, although the short  $T_2^*$  values associated with high sucrose phantoms could be problematic for applications requiring long readout durations or echo times. Furthermore, a phantom with tuned dielectric properties and relaxation times may be valuable for comprehensive MRI coil and pulse sequence evaluation. Although phantoms with tuned relaxation times have been developed,<sup>23–25</sup> the coupled nature of dielectric and relaxation properties may necessitate a complex recipe to simultaneously achieve the desired conductivity, permittivity, and  $T_1$  and  $T_2$  (for example, Gd-based relaxation agents increase conductivity and reduce relaxation times).

One potential disadvantage of sucrose is that its multipeak spectra can confound proton-resonance-frequency MRI thermometry. Similar to the behavior described in water–lipid environments,<sup>26</sup> the water–sucrose spectrum results in a complex nonlinear relationship between temperature and signal phase, which is further modulated by echo time. It is therefore essential to account for this relationship in the interpretation of MR thermometry data, particularly in low permittivity phantoms with high sucrose levels. Another drawback is that the dielectric properties of tissues such as adipose tissue or bone cannot be represented with the developed recipe due to sucrose solubility limits. Similarly, the nominal conductivity of water at high frequencies (higher than used in typical MRI applications) exceeds that of tissues with intermediate conductivity and prevents the replication of tissues such as muscle and gray matter above  $\sim 1.4$  GHz.

The cost of the proposed recipe is low due to the choice of sucrose in terms of table sugar without sacrificing the purity. Based on United States law<sup>27</sup> and international standard,<sup>28</sup>

commercially available granulated pure cane sugar should contain at least 99.5% of sucrose. For the recipe presented here, the cost of distilled water, NaCl, sucrose, agar, and benzoic acid is about \$0.26/l, \$0.02/g, \$0.0014/g, \$0.26/g, and \$2.63/g, respectively. In this case, the costs would be \$5.52/l for 7 T muscle phantom and \$5.06/l for the 11.7 T brain phantom. The cost can be further reduced to \$3.97/l and \$3.71/l if a cheaper benzoic acid (e.g., Benzoic acid AC221800010, 99.5%, for analysis, Acros Organics, New Jersey) is used. The phantoms based on the proposed recipe maintain stable dielectric properties for at least several months, provided that their containers are properly sealed to minimize evaporative losses, and they are stored at room temperature.

Regarding the stability of the proposed phantom, it should be pointed out that there is potential for degradation due to excessive heating. For example, temperatures well above 50 °C may cause melting or even boiling and caramelizing, all of which may affect electrical, thermal, and NMR properties. Fortunately, this is generally not a problem in MRI safety evaluations in which the heating is relatively slow (~1–2 °C/min) and limited (usually with maximum temperature less than 30 °C).

## 5. CONCLUSION

A generic recipe for sucrose–NaCl-based gel phantoms that mimic tissue dielectric properties at low cost (~\$5/l) was generated by systematically characterizing the nonlinear and interdependent relations between the solvents and the resulting dielectric properties. The availability of this recipe will facilitate estimation of wavelength effects on MRI pulse sequence and RF coil performance, tissue heating at high-field strength as well as other applications requiring tissue-mimicking phantoms.

## ACKNOWLEDGMENTS

This research was supported by the Intramural Research Program of the National Institute of Neurological Disorders and Stroke and NIH R01 EB002568.

<sup>a)</sup> Author to whom correspondence should be addressed. Electronic mail: Qi.Duan@nih.gov

<sup>1</sup>H. Merkle, J. Murphy-Boesch, P. Gelderen, S. Wang, T. Q. Li, A. P. Koretsky, and J. H. Duyn, “Transmit B(1) -field correction at 7 T using actively tuned coupled inner elements,” *Magn. Reson. Med.* **66**, 901–910 (2011).

<sup>2</sup>R. Brown, C. M. Deniz, B. Zhang, G. Chang, D. K. Sodickson, and G. C. Wiggins, “Design and application of combined 8-channel transmit and 10-channel receive arrays and radiofrequency shimming for 7-T shoulder magnetic resonance imaging,” *Invest. Radiol.* **49**(1), 35–47 (2014).

<sup>3</sup>L. Alon, C. M. Deniz, R. Brown, D. K. Sodickson, and Y. Zhu, “Method for in situ characterization of radiofrequency heating in parallel transmit MRI,” *Magn. Reson. Med.* **69**, 1457–1465 (2014).

<sup>4</sup>M. A. Cloos, L. Anon, G. Chen, G. C. Wiggins, and D. Sodickson, “Rapid RF safety evaluation for transmit-array coils,” in *21th Annual Meeting & Exhibition of ISMRM* (International Society for Magnetic Resonance in Medicine, Salt Lake City, Utah, 2013), p. 286.

<sup>5</sup>S. Gabriel, R. W. Lau, and C. Gabriel, “The dielectric properties of biological tissues: II. Measurements in the frequency range 10 Hz to 20 GHz,” *Phys. Med. Biol.* **41**, 2251–2269 (1996).

<sup>6</sup>S. Gabriel, R. W. Lau, and C. Gabriel, “The dielectric properties of biological tissues: III. Parametric models for the dielectric spectrum of tissues,” *Phys. Med. Biol.* **41**, 2271–2293 (1996).

<sup>7</sup>H. Kato and T. Ishida, “Development of an agar phantom adaptable for simulation of various tissues in the range 5–40 MHz,” *Phys. Med. Biol.* **32**, 221–226 (1987).

<sup>8</sup>Y. Okano, K. Ito, I. Ida, and M. Takahashi, “The SAR evaluation method by a combination of thermographic experiments and biological tissue-equivalent phantoms,” *IEEE Trans. Microw. Theory Tech.* **48**, 2094–2103 (2000).

<sup>9</sup>K. Ito, K. Furuya, Y. Okano, and L. Hamada, “Development and characteristics of a biological tissue-equivalent phantom for microwaves,” *Electron. Commun. Japan* **1** **84**, 67–77 (2001).

<sup>10</sup>N. N. Graedel, J. R. Polimeni, B. Guerin, B. Gagoski, and L. L. Wald, “An anatomically realistic temperature phantom for radiofrequency heating measurements,” *Magn. Reson. Med.* (epub ahead of publication) (2014).

<sup>11</sup>C.-K. Chou, G.-W. Chen, A. W. Guy, and K. H. Luk, “Formulas for preparing phantom muscle tissue at various radiofrequencies,” *Bioelectromagnetics* **5**, 435–441 (1984).

<sup>12</sup>K. Fukunaga, S. Watanabe, H. Asou, and K. Sato, “Dielectric properties of non-toxic tissue-equivalent liquids for radiowave safety tests,” in *2005 IEEE International Conference on Dielectric Liquids, Coimbra, Portugal, 2005* (IEEE, 2005), pp. 425–428.

<sup>13</sup>V. Lopresto, R. Pinto, R. Lodato, G. A. Lovisolò, and M. Cavagnaro, “Design and realisation of tissue-equivalent dielectric simulators for dosimetric studies on microwave antennas for interstitial ablation,” *Phys. Med.* **28**, 245–253 (2012).

<sup>14</sup>Y. Yuan, C. Wyatt, P. Maccarini, P. Stauffer, O. Craciunescu, J. Macfall, M. Dewhurst, and S. K. Das, “A heterogeneous human tissue mimicking phantom for RF heating and MRI thermal monitoring verification,” *Phys. Med. Biol.* **57**, 2021–2037 (2012).

<sup>15</sup>M. Lazebnik, E. L. Madsen, G. R. Frank, and S. C. Hagness, “Tissue-mimicking phantom materials for narrowband and ultrawideband microwave applications,” *Phys. Med. Biol.* **50**, 4245–4258 (2005).

<sup>16</sup>G. Hartsgröve, A. Kraszewski, and A. Surowiec, “Simulated biological materials for electromagnetic radiation absorption studies,” *Bioelectromagnetics* **8**, 29–36 (1987).

<sup>17</sup>M. Y. Kanda, M. Ballen, S. Salins, C. Chung-Kwang, and Q. Balzano, “Formulation and characterization of tissue equivalent liquids used for RF densitometry and dosimetry measurements,” *IEEE Trans. Microwave Theory Tech.* **52**, 2046–2056 (2004).

<sup>18</sup>C. Akgun, L. DelaBarre, C. J. Snyder, G. Adriany, A. Gopinath, K. Ugurbil, and J. T. Vaughan, “RF field profiling through element design for high field volume coils,” in *ISMRM ESMRMRB Joint Annual Meeting* (International Society for Magnetic Resonance in Medicine, Stockholm Sweden, 2010), p. 243.

<sup>19</sup>M. Asadi, *Beet-Sugar Handbook* (John Wiley & Sons, Hoboken, New Jersey, 2007).

<sup>20</sup>T. Onishi and S. Uebayashi, “Biological Tissue-Equivalent Phantoms Usable in Broadband Frequency Range,” *NTT DoCoMo Tech. J.* **7**, 61–65 (2006).

<sup>21</sup>T. Onishi, R. Ishido, T. Takimoto, K. Saito, S. Uebayashi, M. Takahashi, and K. Ito, “Biological tissue-equivalent agar-based solid phantoms and SAR estimation using the thermographic method in the range of 3–6 GHz,” *IEICE Trans. Commun.* **E88-B**, 3733–3741 (2005).

<sup>22</sup>M. P. Longinotti, M. F. Mazzobre, M. P. Buera, and H. R. Corti, “Effect of salts on the properties of aqueous sugar systems in relation to biomaterial stabilization Part 2. Sugar crystallization rate and electrical conductivity behavior,” *Phys. Chem. Chem. Phys.* **4**, 533–540 (2002).

<sup>23</sup>Y. Ikemoto, W. Takao, K. Yoshitomi, S. Ohno, T. Harimoto, S. Kanazawa, K. Shibuya, M. Kuroda, and H. Katoa, “Development of a human-tissue-like phantom for 3.0-T MRI,” *Med. Phys.* **38**, 6636–6342 (2011).

<sup>24</sup>D. Mustafi, B. Peng, M. Heisen, A. M. Wood, J. Buurman, and G. S. Karczmar, “World of phantoms: Reference standards for bench to breast MRI,” in *17th Annual Meeting & Exhibition of ISMRM* (International Society for Magnetic Resonance in Medicine, Honolulu, Hawaii, 2009), p. 2104.

<sup>25</sup>K. Yoshimura, H. Kato, M. Kuroda, A. Yoshida, K. Hanamoto, A. Tanaka, M. Tsunoda, S. Kanazawa, K. Shibuya, S. Kawasaki, and Y. Hiraki, “Development of a tissue-equivalent MRI phantom using carrageenan gel,” *Magn. Reson. Med.* **50**, 1011–1017 (2003).

<sup>26</sup>J. A. de Zwart, F. C. Vimeux, C. Delalande, P. Canioni, and C. T. Moonen, “Fast lipid-suppressed MR temperature mapping with echo-shifted gradient-echo imaging and spectral-spatial excitation,” *Magn. Reson. Med.* **42**, 53–59 (1999).

<sup>27</sup>J. Westervelt, *American Pure Food and Drug Laws* (Vernon Law Book Co., Kansas City, MO, 1912).

<sup>28</sup>CODEX, Codex standard for sugars, 1999.